GRP94 (gp96) and GRP94 *N*-Terminal Geldanamycin Binding Domain Elicit Tissue Nonrestricted Tumor Suppression

Julie C. Baker-LePain,[1] Marcella Sarzotti,[2] Timothy A. Fields,[3] Chuan-Yuan Li,[4] and Christopher V. Nicchitta[1]

[1]*Department of Cell Biology,* [2]*Department of Immunology,* [3]*Department of Pathology, and* [4]*Department of Radiation Oncology, Duke University Medical Center, Durham, NC 27710*

Abstract

In chemical carcinogenesis models, GRP94 (gp96) elicits tumor-specific protective immunity. The tumor specificity of this response is thought to reflect immune responses to GRP94-bound peptide antigens, the cohort of which uniquely identifies the GRP94 tissue of origin. In this study, we examined the apparent tissue restriction of GRP94-elicited protective immunity in a 4T1 mammary carcinoma model. We report that the vaccination of BALB/c mice with irradiated fibroblasts expressing a secretory form of GRP94 markedly suppressed 4T1 tumor growth and metastasis. In addition, vaccination with irradiated cells secreting the GRP94 NH_2-terminal geldanamycin-binding domain (NTD), a region lacking canonical peptide-binding motifs, yielded a similar suppression of tumor growth and metastatic progression. Conditioned media from cultures of GRP94 or GRP94 NTD-secreting fibroblasts elicited the up-regulation of major histocompatibility complex class II and CD86 in dendritic cell cultures, consistent with a natural adjuvant function for GRP94 and the GRP94 NTD. Based on these findings, we propose that GRP94-elicited tumor suppression can occur independent of the GRP94 tissue of origin and suggest a primary role for GRP4 natural adjuvant function in antitumor immune responses.

Key words: chaperone • heat shock protein • dendritic cell • cancer • immunotherapy

Introduction

GRP94 (gp96) elicits antitumor responses in prophylactic and therapeutic immunization protocols (1–4). This phenomenon, discovered by Srivastava and co-workers (1–3) in a methylcholanthrene-elicited fibrosarcoma model, displays stringent tissue restriction. To explain the absence of cross protection, it was proposed that GRP94 binds antigenic peptides, thereby endowing the protein with the immunological identity of its tissue of origin, and can be processed by professional APCs to yield tumor-directed adaptive immune responses (1, 5). In support of this proposal, in vitro generated complexes of GRP94 and known peptide antigens have been demonstrated to undergo receptor-mediated uptake by APC with subsequent representation of the GRP94-associated peptides on APC MHC class I molecules (6–13).

In addition to its capacity to direct peptides into the class I antigen presentation pathway, GRP94 displays the properties of a natural adjuvant in its interactions with cells of the innate immune system. For example, GRP94 as well as other heat shock/chaperone proteins activate nuclear factor (NF)*-κB–mediated signal transduction and cytokine production in APCs and importantly, promote the phenotypic maturation of dendritic cells (DCs; 14–19). Such activities are not dependent upon the presence of associated tumor-specific antigens, as they occur with proteins derived from nontumor tissues (14–19). These functions are likely relevant to the ability of GRP94 to modulate immune responses, as it is now thought that the activation of innate immunity is an essential regulatory element in the processes leading to the generation of antigen-specific adaptive immunity (20).

Address correspondence to Christopher V. Nicchitta, Department of Cell Biology, Duke University Medical Center, 366 Nanaline H. Duke, Durham, NC 27710. Phone: 919-684-8948; Fax: 919-684-5481; E-mail: c.nicchitta@cellbio.duke.edu

**Abbreviations used in this paper:* DC, dendritic cell; Endo H, endoglycosidase H; NF, nuclear factor; NTD, NH_2-terminal geldanamycin-binding domain; PNGase-F, peptide *N*-glycosidase F; TR, Texas red.

 J. Exp. Med. © The Rockefeller University Press • 0022-1007/2002/12/1447/13 $5.00
Volume 196, Number 11, December 2, 2002 1447–1459
http://www.jem.org/cgi/doi/10.1084/jem.20020436

Although it is well established that GRP94 can elicit tumor suppression, the precise immunological basis for this phenomenon, in particular the relative contribution of the innate and adaptive components of the cellular immune response, is unknown. We examined this question in a 4T1 murine mammary carcinoma prophylactic vaccination model. To address the requirement for tissue restriction, irradiated cells (4T1 mammary carcinoma, NIH-3T3 fibroblast, and KBALB fibroblast) expressing a secretory form of GRP94 were used in the vaccination stage before challenge with 4T1 cells. Paired vaccination studies were also performed using cells (4T1 or KBALB) expressing a secretory form of the GRP94 NH_2-terminal geldanamycin-binding domain (NTD), which lacks canonical peptide binding motifs. We report that vaccination with 4T1, NIH-3T3, or KBALB cells secreting either GRP94 or the GRP94 NTD yielded a pronounced suppression of 4T1 tumor growth and metastatic progression. In vitro, tissue culture supernatants of cells secreting GRP94 or its NH_2-terminal domain were a stimulus for the up-regulation of DC MHC class II and CD86 expression. Combined, these results indicate that GRP94-mediated tumor suppression can occur independent of the GRP94 tissue of origin and suggest a natural adjuvant function for GRP94 in the etiology of GRP94-elicited antitumor immune responses.

Materials and Methods

Reagents. Pro-mix ([^{35}S]methionine and [^{35}S]cysteine) was obtained from Amersham Biosciences. Endoglycosidase H (Endo H) was purchased from Boehringer. Peptide *N*-glycosidase F (PNGase-F) was purchased from New England Biolabs, Inc. Cell culture media and reagents were from GIBCO BRL. All other reagents were purchased from Sigma-Aldrich unless noted otherwise.

Mice. Female BALB/c mice (H-2^d) were obtained from Charles River Laboratories. Female C57BL/6 mice (H-2^b) were obtained from National Cancer Institute Frederick Cancer Research and Development Center. Animals were maintained and treated in strict accordance with all applicable Institutional and Animal Care Use Committee animal care guidelines.

Antibodies and Cell Lines. Antipeptide antiserum against GRP94 NH_2-terminal peptide (DU-120) was prepared according to the protocol of Harlow and Lane (21), with antibody production performed by contract supplier (Cocalico Biologicals). Monoclonal antibody to the myc epitope (9E10) was purchased from Zymed Laboratories. Antibody to prolactin was purchased from Research Diagnostics. PE-conjugated anti–mouse I-A^b, CD86, GR-1, and CD11c and FITC-conjugated anti–mouse CD40 and CD80 and appropriate isotype controls were purchased from BD Biosciences. NIH-3T3 (H-2^q), K-BALB (H-2^d), RAW264.7 (H-2^d), B16-F10 (H-2^b), and COS-7 cells were obtained from American Type Culture Collection. 4T1 cells (H-2^d) were obtained from F. Miller, Michigan Cancer Foundation, Detroit, MI. 4T1, NIH-3T3, K-BALB, RAW264.7, and B16-F10 cells were cultured in DME supplemented with 10% fetal calf serum, 100 U/ml penicillin, and 100 μg/ml streptomycin. All cell lines tested negative for mycoplasma DNA.

Construct Preparation. Canine GRP94 cDNA was used as the template for all PCR reactions. For GRP94ΔKDEL, the 5′ sense primer (5′ GCGTCGACAGGGCCCTGTGGGTGCTG 3′) and the 3′ antisense primer (5′ GCGCGGCCGCTCATTCAGA TGTAGATTTCTT 3′) were used to prepare a PCR product corresponding to the 5′ 2,403 bp of the GRP94 coding region flanked by 5′ SalI and 3′ NotI restriction sites. The PCR product was digested with SalI/NotI and ligated into SalI/NotI-digested pEF/myc/cyto (Invitrogen). For GRP94 NTD, the 5′ sense primer (5′ GCGTCGACAGGGCCCTGTGGGTGCTG 3′) and the 3′ antisense primer (5′ GCGCGGCCGCTCAATTCATAAGC TCCCAATCCCA 3′) were used to prepare a PCR product corresponding to the 5′ 1,111 bp of the GRP94 coding region flanked by 5′ SalI and 3′ NotI restriction sites. The PCR product was digested with SalI/NotI and ligated into SalI/NotI-digested pEF/myc/cyto vector. GRP94 NTD for recombinant expression was prepared using the 5′ sense primer (5′ GGAATTCCATATG-GACGATGAAGTCGATGTG 3′) and the 3′ antisense primer (5′ CGGATCCTCAATTCATAAGCTCCCAATCCCA 3′) to obtain a PCR product corresponding to bp 64–1,008 of the GRP94 coding sequence, flanked by 5′ NdeI and 3′ BamHI restriction sites. The PCR product was digested with NdeI/BamHI and ligated into NdeI/BamHI-digested pGEX vector (provided by D. Gewirth, Duke University Medical Center, Durham, NC). Preparation of the preprolactin construct has been previously described (22).

Protein Expression and Purification. GRP94 was purified from porcine pancreas as previously described (23). Recombinant GRP94 NTD protein was expressed in *E. coli* strain BL21 and purified using a GSTrap affinity column (Amersham Biosciences) according to the manufacturer's instructions. Removal of glutathione *S*-transferase was accomplished by thrombin digestion according to manufacturer's instructions. Additional purification was performed using Superdex 75 gel filtration chromatography (Amersham Biosciences). GRP94 or recombinant GRP94 NTD was labeled with FITC or Texas Red (TR) (Molecular Probes Inc.) to a ratio of 2 or 3 mol dye/mol protein according to the manufacturer's instructions. In studies of cell surface binding and trafficking, TR-GRP94 and FITC-GRP94 NTD were present at equimolar concentrations.

Transfections. All transfections were performed using Lipofectamine™ reagent (GIBCO BRL) according to the manufacturer's instructions. Mock transfections were performed with serum-free DME or with pEF/myc/cyto vector plus Lipofectamine™. For the preparation of conditioned media, cells were transfected for 5 h in serum-free DME plus DNA and Lipofectamine™. Cells were then rinsed gently with sterile PBS and transferred to DC culture media. After 72 h of culture, media were collected and subjected to low speed centrifugation to yield a cell-free supernatant fraction. These media were diluted 1:1 with fresh DC culture media and applied to day 6 DCs, as described below.

Immunofluorescence. 4T1 cells were grown on glass coverslips in 6-well plates overnight to 50% confluence. Cells were then fixed in 4% paraformaldehyde in PBS for 10 min on ice, permeabilized in 0.1% Triton X-100 in PBS for 15 min on ice, and blocking was performed by incubation in 1% BSA in PBS for 30 min at room temperature. For analysis of myc tag–bearing expression products, incubations were performed with a 1:200 dilution of anti-myc antibody in 0.1% BSA in PBS for 1 h at room temperature. After extensive washing, bound antibodies were labeled by incubation in a 1:200 dilution of TR-conjugated goat anti–mouse antibody (Cappel Laboratories) in 0.1% BSA in PBS for 1 h at room temperature. After washing, coverslips were mounted onto glass slides using mounting media (Difco Laboratories). Trafficking studies were performed using

thioglycollate-elicited C57BL/6 peritoneal macrophages. Macrophages were adherence selected for 1 h at 37°C. Cell surface binding was performed by incubation with fluorophore-labeled proteins for 1 h at 4°C in RPMI plus 10% fetal calf serum. After binding, cells were washed extensively with ice-cold RPMI. After the final wash, cells were exchanged into prewarmed RPMI plus 10% fetal calf serum and incubated at 37°C for the indicated times. To stop transport, cells were rapidly washed in ice-cold Hepes-buffered saline (0.8% NaCl, 25 mM K-Hepes, pH 7.2, 1 mM $CaCl_2$, 0.5 mM $MgCl_2$) and fixed in 4% paraformaldehyde in PBS for 10 min on ice. Cells were washed again and mounted onto glass slides using mounting media (Difco Laboratories). Confocal microscopy sections were obtained using a Zeiss LSM-410 confocal microscope. All images were processed using Adobe Photoshop® Version 6.0 software.

Pulse-Chase Studies, Immunoprecipitation, and Glycosidase Digestions. 24 h after transfection, cells were incubated in serum-, methionine-, and cysteine-free DME at 37°C for 20 min and then pulse labeled by incubation in serum-, methionine-, and cysteine-free DME supplemented with 100 μCi/ml [^{35}S]-labeled pro-mix at 37°C for 30 min. Cells were then washed and incubated in chase medium (growth medium plus 1 mM unlabeled L-methionine) at 37°C for the indicated times. Samples of chase media were collected and cleared by brief centrifugation (10 min, 15,000 *g*). Cells were lysed in ice-cold lysis buffer (150 mM NaCl, 50 mM Tris, pH 7.5, 0.05% SDS, 1% NP-40) and cleared by centrifugation (10 min, 15,000 *g*). Chase media and lysate samples were precleared with normal mouse serum and Pansorbin cells (Calbiochem). Proteins were immunoprecipitated from precleared samples using anti-GRP94 (DU-120) or anti-myc (9E10) antibodies and protein A–Sepharose beads. Immunoprecipitates were processed for SDS-PAGE and resolved on 6, 10, or 12.5% gels. For analysis of N-linked oligosaccharide composition, samples were incubated in denaturing buffer (0.5% SDS, 1% 2-mercaptoethanol) at 100°C for 10 min. For Endo H digestions, denatured proteins were incubated in G5 buffer (50 mM sodium citrate, pH 5.5) with or without 5 mU Endo H at 37°C for 2.5 h. For PNGase-F digestions, denatured proteins were incubated in G7 buffer (50 mM sodium phosphate, pH 7.5) plus 1% NP-40 with or without 0.8 mU PNGase-F at 37°C for 2.5 h. Samples were then processed for SDS-PAGE and resolved on 6% polyacrylamide gels. Radiolabeled proteins were visualized by PhosphorImager analysis (Fuji Medical Systems) using MacBAS-2.0® software.

In Vivo Tumor Studies. Transfected 4T1, NIH-3T3, or KBALB cells were prepared as described above and irradiated (10,000 rad) 24 h after transfection. Irradiated cells were washed extensively with sterile PBS and vaccination was performed by intradermal injections of 2–4 × 10^6 cells into the left hindlimb skin of BALB/c mice. Immunizations were given weekly for four consecutive weeks. On week 5, mice were challenged with 10^6 4T1 cells in sterile PBS by intradermal injection into the right back. Tumor length, width, and height were measured every 2–3 d after challenge, and tumor volume was calculated using the following formula: Volume = (π/6) × length × width × height. At the completion of the study, animals were killed, and lungs were resected and weighed. Tumors were excised and submerged in 10% neutral buffered formalin solution. Paraffin embedding, tissue sectioning, and histological staining with hematoxylin and eosin were performed by the Duke University Histology Laboratory. Statistical comparisons were performed using the Wilcoxon rank sum test (n = 8–10 animals).

Generation of Bone Marrow–derived DCs. Bone marrow–derived DCs were propagated from bone marrow progenitor cells according to the method of Inaba et al. (24) with minor modifications. Bone marrow precursors flushed from the tibiae and femurs of C57BL/6 mice were plated at 10^6 cells/ml in DC culture media (RPMI 1640 plus 5% heat-inactivated fetal calf serum, 100 U/ml penicillin, 100 μg/ml streptomycin, 20 μg/ml gentamicin, 50 μM 2-mercaptoethanol) supplemented with GM-CSF (5% culture supernatant from X63 cells stably transfected with murine GM-CSF cDNA). Cultures were washed on days 2 and 4. For maturation assays, day 6 DCs were harvested and transferred to fresh 6-well plates at 5 × 10^5 cells/ml after resuspension in the appropriate control media or conditioned media. Cells were harvested on day 7 and Fc receptors were blocked with Fc-block® reagent (BD Biosciences) before staining with antibody. After fixation, cells were analyzed by flow cytometry using FACScan® and CellQuest® software.

Cell Surface Binding Assay. Cells, either adherent or in suspension culture, were incubated with recombinant fluorescein-labeled GRP94 NTD in complete media for 1 h at 4°C. After washing with ice-cold media and PBS, cells were fixed with 4% paraformaldehyde and analyzed by flow cytometry using FACScan™ and CellQuest™ software.

Results

Experimental System. To date, studies on the mechanism of GRP94-elicited tumor rejection have primarily used GRP94 prepared by chromatographic fractionation of tissue or cell homogenates. With such preparations come concerns regarding protein purity, particularly where an immunological response is the experimental endpoint (25–27). This concern is especially relevant to heat shock/chaperone proteins, which because of their abundance, typically undergo relatively modest enrichment (<20-fold) during purification (23, 25–27). As an alternative to vaccination with biochemically enriched GRP94 fractions, we used an experimental system in which cells were transfected with vectors encoding secretory forms of GRP94 and were used as vaccines in a prophylactic immunotherapy model. By varying the vector host tissue, we examined the hypothesis that GRP94-mediated tumor rejection is tissue restricted.

Processing and Secretion of GRP94. A secretory form of GRP94 was engineered by deletion of its KDEL ER retention/retrieval sequence (28) to yield GRP94ΔKDEL. To distinguish GRP94ΔKDEL from endogenous GRP94, a myc tag was encoded in the COOH terminus. After transfection of 4T1 breast carcinoma cells, GRP94ΔKDEL processing and secretion was examined. As shown in Fig. 1 A, cells expressing GRP94ΔKDEL displayed a robust ER/Golgi staining pattern. No myc-reactive staining was observed after transfection with vector alone (unpublished data). Pulse-chase studies were performed to examine GRP94ΔKDEL secretion. As shown in Fig. 1 B, media samples from GRP94ΔKDEL-transfected 4T1 cells contained a doublet of proteins of 100 and 110 kD, recognized by both the anti-myc and anti-GRP94 antibodies. Supernatants of mock-transfected cells yielded neither component (Fig. 1 B). The 100/110 kD GRP94 doublet was also present in radiolabeled cell lysate fractions. As expected, cell lysates of both GRP94ΔKDEL-transfected and mock-

transfected cells contained a protein species corresponding to endogenous GRP94 (Fig. 1 B, *).

We postulated that the presence of the 100/110 kD doublet reflected heterogeneous oligosaccharide processing of GRP94ΔKDEL during transit through the Golgi apparatus. To test this hypothesis, immunoprecipitates of chase media of cell lysates from GRP94ΔKDEL-transfected cells were digested with Endo H or PNGase-F. As depicted in Fig. 1 C, the protein doublet present in both chase media and cell lysates resolved to a single protein species upon digestion with PNGase-F (lanes 5–8). Endogenous GRP94 in cell lysates shifted to a higher mobility position upon PNGase-F digestion but remained distinct from GRP94ΔKDEL species. This difference in mobility between GRP94ΔKDEL and endogenous GRP94 likely reflects the presence of the myc tag on the former. Endo H, an enzyme that cleaves high mannose oligosaccharides representative of the ER and early Golgi, did not alter the doublet present in the secreted GRP94ΔKDEL, but resolved that present in the cell lysates to a single species (Fig. 1 C, lanes 1–4).

Deletion of the KDEL retention/retrieval sequence of ER resident lumenal proteins allows secretion, albeit often at markedly slower rates than that observed in bona fide secretory proteins (29). To assess the relative rate of GRP94ΔKDEL secretion, pulse-chase studies were performed on 4T1 cells that had been transfected with constructs encoding either GRP94ΔKDEL or the model secretory hormone preprolactin. As shown in Fig. 2, GRP94ΔKDEL secretion is efficient, with a half-time of 2 h versus 1 h for native preprolactin. Interestingly, endogenous GRP94, seen as a distinct band in immunoprecipitates of cell lysates, remained at constant levels over time, indicating that heterodimerization of full-length GRP94 with GRP94ΔKDEL was not a significant competing assembly reaction.

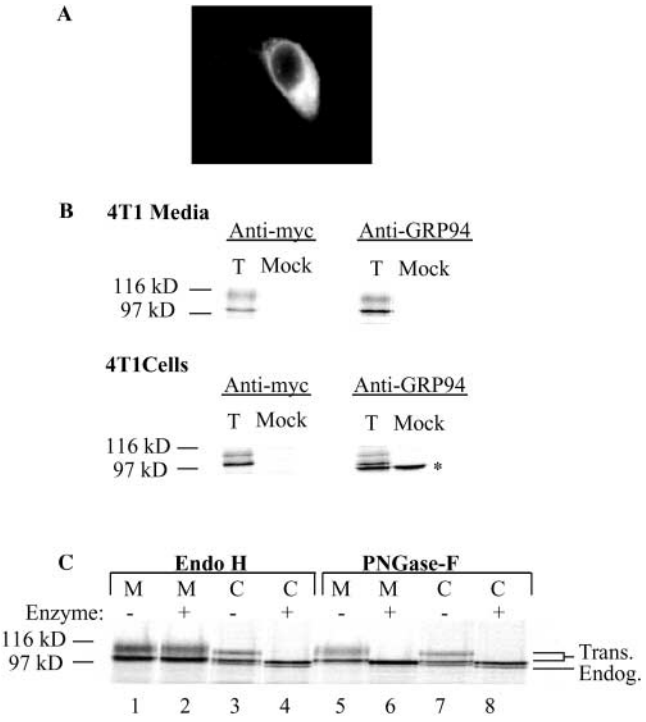

Figure 1. GRP94ΔKDEL is secreted by transfected 4T1 mammary carcinoma cells. (A) Immunofluorescence with anti-myc antibody reveals expression of GRP94ΔKDEL within transfected 4T1 cells. 4T1 cells were grown on glass coverslips and stained with anti-myc antibody (9E10) and TR-conjugated secondary antibody, and then visualized by confocal microscopy (100×). (B–C) Oligosaccharide processing of GRP94ΔKDEL. Media or cell lysates from mock-transfected (mock) or GRP94ΔKDEL-transfected (T) 4T1 cells were collected after metabolic labeling with [^{35}S]Promix. GRP94 species were recovered by immunoprecipitation with either anti-GRP94 antibody or anti-myc antibody, as indicated. GRP94ΔKDEL appears as a doublet of bands distinct from endogenous, full-length GRP94 (*). (C) Glycosidase digestion of GRP94ΔKDEL. Media (M) or cell lysates (C) from GRP94ΔKDEL-transfected 4T1 cells were collected as described in B and then treated (+) or not treated (−) with Endo H or PNGase-F, as indicated. Endogenous GRP94 in the cell lysate samples (position "E") and transfected forms of GRP94 are indicated ("T" positions). All samples were resolved by SDS-PAGE on 6% gels and visualized by PhosphorImager analysis.

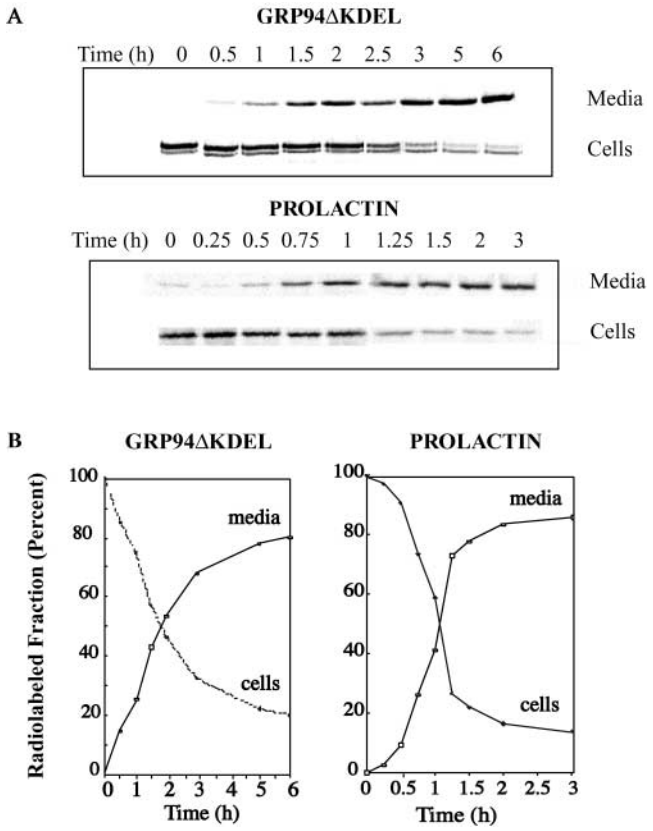

Figure 2. Kinetics of GRP94ΔKDEL secretion from 4T1 breast carcinoma cells. (A) 4T1 cells were metabolically labeled with [^{35}S]Promix and then media and cell lysates were collected and immunoprecipitated with anti-GRP94 antibody. All samples were treated with PNGase-F before resolution by SDS-PAGE on 6% gels for GRP94ΔKDEL or 10% gels for prolactin. Radiolabeled proteins were visualized by PhosphorImager analysis. (B) Bands from A were quantified using MacBAS-2.0 software and were used to determine percent total GRP94ΔKDEL or prolactin present in the media or cell lysate at each time point.

Vaccination with GRP94ΔKDEL-secreting 4T1 Mammary Carcinoma Cells or GRP94ΔKDEL-secreting NIH-3T3 Fibroblasts Suppresses 4T1 Tumor Growth. To examine the contribution of the GRP94 tissue of origin to the phenomenon of GRP94-dependent tumor suppression, we used the 4T1 tumor model. 4T1 cells, derived from a spontaneous mammary carcinoma of the BALB/c mouse, are highly aggressive and metastasize widely (30). To ensure that the cells used in the vaccination phase did not establish tumors, cells were irradiated before injection into animals. As shown in Fig. 3 A, irradiation did not compromise the ability of the cells to synthesize or secrete GRP94ΔKDEL.

To determine whether secretion of GRP94 could elicit antitumor responses, mice were immunized with irradiated, GRP94ΔKDEL-transfected 4T1 cells before challenge with viable 4T1 cells. In these experiments, control groups were immunized with either PBS or irradiated, mock-transfected 4T1 cells (4T1-mock). As expected, mice in both control groups displayed rapid tumor growth upon challenge with 4T1 tumor cells. Mock-transfected 4T1 cells were weakly immunogenic. The difference in tumor volumes between the PBS-immunized and the 4T1-mock–immunized groups was not, however, statistically significant ($P \leq 0.33$; Fig. 3, B, C, and G). In contrast, mice immunized with GRP94ΔKDEL-secreting 4T1 cells (4T1-ΔKDEL) displayed a reduced rate of tumor growth (Fig. 3, B, D, and G). The difference in tumor volumes between this group and the control groups was statistically significant ($P \leq 0.00005$ for PBS vs. 4T1-ΔKDEL and $P \leq 0.010$ for 4T1-mock vs. 4T1-ΔKDEL; Fig. 3 G).

Having established that prophylactic vaccination of mice with irradiated, GRP94-secreting 4T1 cells was sufficient to elicit tumor suppression, we examined the role of the GRP94ΔKDEL cell host in the elicitation of tumor suppression. In one series of experiments, an allogenic fibroblast cell line (NIH-3T3) was used as the vector cell host. Pulse-chase studies comparing the relative GRP94ΔKDEL secretion capacities of 4T1 and NIH-3T3 cells revealed that both cell types secreted similar levels of GRP94ΔKDEL (unpublished data). Vaccination with irradiated, mock-transfected NIH-

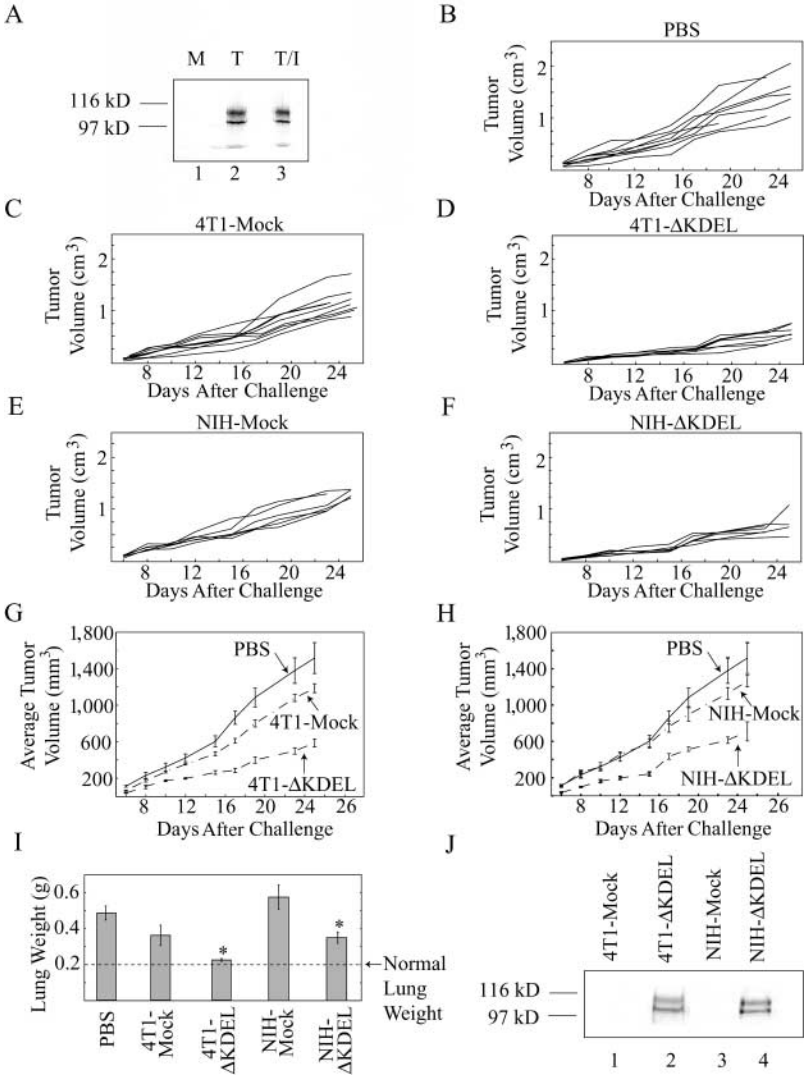

Figure 3. Vaccination with 4T1 mammary carcinoma cells or NIH-3T3 fibroblasts secreting GRP94ΔKDEL leads to delayed tumor growth rates and decreased tumor metastasis. (A) Irradiation does not alter the secretion of GRP94ΔKDEL. 4T1 cells were transfected with GRP94ΔKDEL (T and T/I) or mock-transfected (mock). 24 h after transfection, cells were irradiated with 10,000 rads (T/I) or left unirradiated (T). 72 h after transfection, cells were metabolically labeled with [^{35}S]Promix and GRP94ΔKDEL was recovered from the media by immunoprecipitation. Proteins were resolved by SDS-PAGE on 6% gels and visualized by PhosphorImager analysis. (B–H) GRP94ΔKDEL secretion from either 4T1 cells or NIH-3T3 fibroblasts elicits delayed tumor growth. Female BALB/c mice were immunized with PBS or with irradiated, GRP94ΔKDEL-transfected or irradiated, mock-transfected 4T1 or NIH-3T3 cells, as indicated. Animals were then challenged with unirradiated 4T1 cells, as described in Materials and Methods, and tumor volumes were followed over time. Tumor growth curves for individual mice in each group are shown in B–F and average tumor volumes with standard error are shown in G and H. (I) GRP94ΔKDEL secretion from either 4T1 cells or NIH-3T3 fibroblasts elicits decreased metastatic tumor progression. After sacrifice, lungs were resected from mice in B–H and weighed to determine the extent of metastatic tumor burden. Average weights with standard error are shown with groups differing significantly from PBS control denoted by an asterisk ($P \leq 0.0012$ for 4T1-ΔKDEL and $P \leq 0.025$ for NIH-ΔKDEL). (J) Comparison of the relative levels of GRP94ΔKDEL secretion by 4T1 and NIH-3T3 cells. Equal numbers (10^6 cells) of 4T1 or NIH3T3 cells were transfected with GRP94ΔKDEL (ΔKDEL samples) or mock-transfected (mock samples). 24 h after transfection, cells were metabolically labeled with [^{35}S]Promix and GRP94DKDEL was recovered from the media by immunoprecipitation. Proteins were resolved by SDS-PAGE on 6% gels and visualized by PhosphorImager analysis.

3T3 cells (NIH-mock) had little effect on subsequent 4T1 tumor growth compared with PBS ($P \leq 0.57$; Fig. 3, B, E, and H). Unexpectedly, animals immunized with GRP94ΔKDEL-secreting NIH-3T3 cells (NIH-ΔKDEL) displayed significantly reduced rates of tumor growth compared with control animals ($P \leq 0.0013$ for PBS vs. NIH-ΔKDEL and $P \leq 0.0022$ for NIH-mock vs. NIH-ΔKDEL; Fig. 3, F and H).

To examine the effects of vaccination on metastatic progression, animals were killed at the conclusion of the study and their lungs were examined for evidence of distal tumor metastasis. Lungs from control animals bore numerous tumor nodules with far fewer nodules seen in GRP94ΔKDEL-treated animals (unpublished data). Lung weights were determined to quantify the extent of tumor metastases (Fig. 3 I). Animals immunized with mock-transfected 4T1 cells demonstrated slightly reduced lung weights compared with PBS-immunized controls, although this difference was not statistically significant ($P \leq 0.070$). In contrast, animals immunized with GRP94ΔKDEL-secreting 4T1 cells displayed a significantly reduced metastatic tumor burden ($P \leq 0.0012$ for PBS vs. 4T1-ΔKDEL and $P \leq 0.010$ for 4T1-mock vs. 4T1-ΔKDEL). Similarly, lung tumor burden in mice immunized with GRP94ΔKDEL-transfected NIH-3T3 fibroblasts was significantly less than those of control mice ($P \leq 0.025$ for PBS vs. NIH-ΔKDEL and $P \leq 0.026$ for NIH-mock vs. NIH-ΔKDEL).

To compare the relative levels of GRP94ΔKDEL secretion by 4T1 and NIH-3T3 cells, pulse-chase experiments were performed (Fig. 3 J). The level of GRP94ΔKDEL secretion by both cell types was comparable, indicating that the tumor suppression observed after immunization with GRP94-secreting fibroblasts does not result from an increased GRP94 dose as compared with GRP94-secreting 4T1 cells.

A Role for GRP94 Structural Domains in DC Maturation and Tumor Suppression. The previous experiments established that vaccination of BALB/c mice with irradiated fibroblasts engineered to secrete GRP94 provided protection, albeit incomplete, against subsequent challenge with 4T1 tumor cells. These findings suggested that GRP94-mediated tumor suppression in this system was not tissue restricted. Alternatively, and perhaps more likely, it was also considered that the GRP94 secreted from NIH-3T3 fibroblasts was complexed with antigens common to 4T1 mammary carcinoma cells, thereby eliciting anti-4T1 cellular immune responses during the immunization stage. We used a protein domain expression strategy to examine this possibility. GRP94, the endoplasmic reticulum Hsp90 paralog, is comprised of three primary structural domains: an NH_2-terminal geldanamycin/adenosine nucleotide binding domain, a middle domain, and a COOH-terminal dimerization domain (31–34). Previously, the putative peptide-binding domain has been mapped to a COOH-terminal region adjacent to the dimerization domain (35). In this study, we investigated the GRP94 NH_2-terminal domain. This domain has been crystallized and as observed with Hsp90, displays a binding pocket for adenosine nucleotides and the antitumor drugs geldanamycin and radicicol (unpublished data). Importantly, this domain lacks canonical peptide-binding motifs.

First, we examined the interaction of GRP94 NTD with APC. As shown in Fig. 4 A, GRP94 NTD displayed cell surface binding to bone marrow–derived DCs, elicited peritoneal macrophages, and the macrophage-derived cell line RAW264.7. Little or no binding of GRP94 NTD was observed in B16-F10 melanoma cells, COS7 kidney cells, or NIH-3T3 fibroblasts. Fluorescently labeled full-length GRP94 similarly displayed binding to DCs, peritoneal macrophages, and RAW264.7 cells with little to no binding to B16-F10, COS7, or NIH-3T3 cells (11 and unpublished data).

As a result of cell surface binding to APCs, GRP94 undergoes receptor-mediated endocytosis (7–10, 13). To investigate the fate of cell surface–bound GRP94 NTD, fluorescently labeled GRP94 or GRP94 NTD was first bound to elicited peritoneal macrophages at 4°C. After binding, unbound protein was removed by washing and the cells were warmed to 37°C. In cells fixed before warming, prominent cell surface binding of both GRP94 and the GRP94 NH_2-terminal domain was observed (Fig. 4 B, 0 min). After 10 min at 37°C, both GRP94 and GRP94 NH_2-terminal domain gained entry to the cell as indicated by a punctate intracellular peri-plasmalemmal staining pattern (Fig. 4 B, 10 min). At longer incubation intervals, GRP94 and GRP94 NH_2-terminal domain were more widely dispersed throughout the cell interior in prominent vesicular structures. At each time point, full-length GRP94 colocalized with the GRP94 NH_2-terminal domain (Fig. 4 B, Overlay). The internalization of GRP94 and GRP94 NH_2-terminal domain was not interdependent. Both proteins were internalized and displayed a similar trafficking pattern in the absence of the other (unpublished data). These observations indicate that the NH_2-terminal domain of GRP94 displays the pattern elements necessary for recognition and clearance by APCs.

GRP94ΔKDEL and GRP94 N-Terminal Domain Secreted from NIH-3T3 Fibroblasts Elicit the Up-regulation of MHC Class II and Costimulatory CD86 on DCs. It has previously been reported that GRP94 purified from normal (nontumor) tissues elicits the up-regulation of MHC class II molecules and costimulatory molecules such as CD86 (B7-2) in DCs (14, 15). To explore the biological relevance of GRP94 NTD recognition by APCs, we examined whether the GRP94 NTD altered the expression of cell surface markers on DCs.

DCs isolated on day 6 of culture displayed the following characteristic phenotype: $CD11c^+$, MHC class II intermediate, GR-1^-, $CD80^{low}$, $CD86^{low}$, $CD40^{low}$ (Fig. 5 A). As expected, incubation of day 6 DCs for an additional 24 h in media containing 100 ng/ml LPS produced the up-regulation of MHC class II, CD80, CD86, and CD40 as compared with incubation in media alone (Fig. 5 B). Incubation of DCs in conditioned media from mock-transfected NIH-3T3 cells produced comparatively little up-regulation of MHC class II, CD80, CD86, and CD40 (Fig. 5 B). Notably, exposure of day 6 DCs to conditioned media from

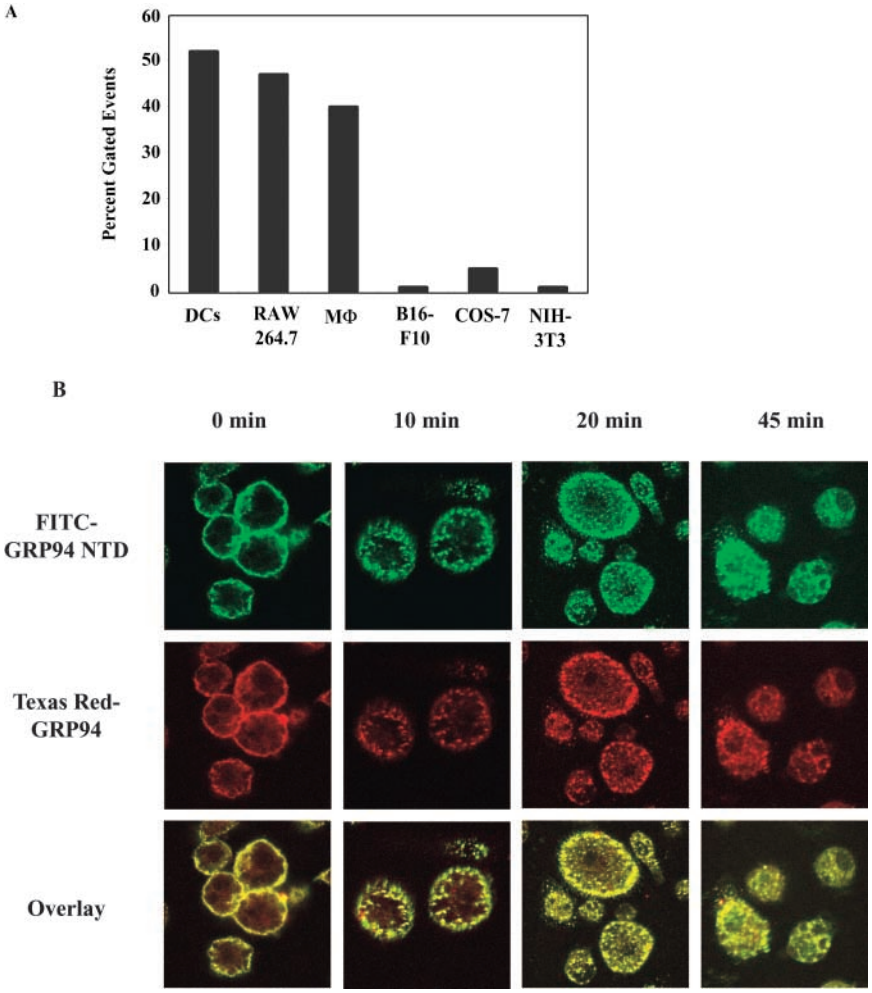

Figure 4. GRP94 NH_2-terminal domain is cleared by APCs and colocalizes with full-length GRP94 upon internalization. (A) Cell type specificity of GRP94 NH_2-terminal domain binding. Recombinantly expressed GRP94 NH_2-terminal domain was fluorescently labeled and used in a standard binding assay with various cell types as described in Materials and Methods. The percentage of cells exhibiting mean fluorescence above control is indicated. (B) Clearance of GRP94 and GRP94 NH_2-terminal regulatory domain by peritoneal macrophages. Elicited peritoneal macrophages were incubated with FITC-labeled GRP94 *N*-terminal domain (FITC-GRP94 NTD) and TR-labeled full-length GRP94 (Texas Red-GRP94). After washing at 4°C to remove unbound protein, cells were warmed to 37°C for the indicated times before fixation and visualization by confocal microscopy (100×). The overlay image displays dual channel imaging of both labeled proteins.

GRP94ΔKDEL-transfected or GRP94 NTD-transfected NIH-3T3 cells yielded the up-regulation of MHC class II and CD86 expression with little effect on CD40 and CD80 expression (Fig. 5 B). This phenotypic pattern has been previously described for exposure to full-length, tissue-purified GRP94 (14, 15). These data indicate that secretory forms of GRP94 and the GRP94 NH_2-terminal domain can recapitulate the function of GRP94 in the promotion of DC maturation.

Immunization with GRP94 N-Terminal Domain Suppresses 4T1 Tumor Growth. The observation that the GRP94 NH_2-terminal domain functioned similarly to the full-length protein in assays of APC cell-surface binding, internalization, and DC maturation indicated that this domain was biologically active. However, it was unknown whether this domain would elicit antitumor immune responses. To determine if the GRP94 NH_2-terminal domain displayed tumor suppression activity, 4T1 cells were transfected with vector-encoding GRP94 NTD cDNA. After transfection, the expression and secretion of a 36-kD protein reactive to antibodies was raised against the NH_2 terminus of GRP94 (Fig. 6 A). In contrast to results obtained with GRP94 ΔKDEL, GRP94 NTD was secreted as a single species, indicating that this domain did not undergo the extensive heterogeneous glycosylation observed for GRP94ΔKDEL (Fig. 6 A).

In vivo tumor studies were performed using irradiated 4T1 cells expressing GRP94 NTD in the vaccination phase (Fig. 6, B–F). As shown in Fig. 6, B–E, mice receiving immunizations of GRP94 NTD-transfected 4T1 cells displayed markedly smaller tumor size and slower tumor growth rates than mice immunized with PBS or mock-transfected cells ($P \leq 0.0002$ for PBS vs. 4T1-GRP94 NTD and $P \leq 0.0006$ for 4T1-mock vs. 4T1-GRP94 NTD; Fig. 6, B–E). In addition, animals immunized with GRP94 NTD-secreting cells displayed significantly reduced lung tumor burden than control animals ($P \leq 0.0031$ for PBS vs. 4T1-GRP94 NTD and $P \leq 0.0008$ for 4T1-mock vs. 4T1-GRP94 NTD).

To extend these observations, vaccination trials were performed with haplotype-matched KBALB fibroblasts transfected with GRP94ΔKDEL or GRP94 NTD cDNA. The results of these studies are depicted in Fig. 7, where it was observed that animals immunized with GRP94 NTD-secreting KBALB cells displayed reduced primary tumor burden than animals immunized with PBS or mock-trans-

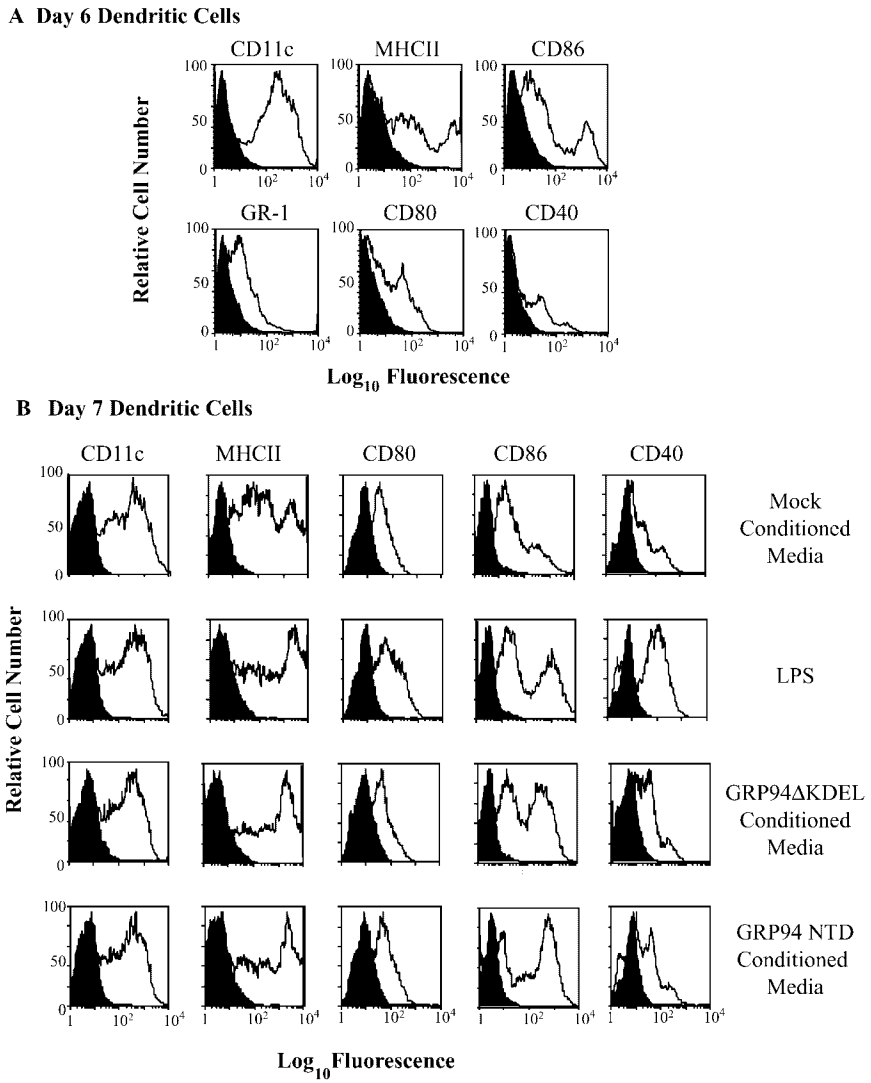

Figure 5. GRP94ΔKDEL and GRP94 *N*-terminal domain elicit DC maturation. Conditioned media from GRP94ΔKDEL-transfected, GRP94 NTD-transfected, or mock-transfected NIH-3T3 cells were collected for 72 h and incubated with day 6 DCs as described in Materials and Methods. (A) Phenotypic profile of day 6 DCs before incubation with conditioned media. (B) Phenotypic profile of day 7 DCs after incubation with conditioned media from mock-transfected, GRP94ΔKDEL-transfected, or GRP94 NTD-transfected NIH-3T3 cells. Incubation in media plus LPS was used as a positive control.

fected cells ($P \leq 0.0003$ for PBS vs. KBALB-GRP94ΔKDEL, $P \leq 0.0003$ for PBS vs. KBALB-GRP94 NTD, and $P \leq 0.24$ for PBS vs. KBALB-Mock; Fig. 7, A–E). In addition, animals immunized with syngeneic fibroblasts secreting GRP94ΔKDEL or GRP94 NTD had decreased metastatic tumor burden ($P \leq 0.0003$ for PBS vs. KBALB-GRP94ΔKDEL, $P \leq 0.0002$ for PBS vs. KBALB-GRP94 NTD, and $P \leq 0.8$ for PBS vs. KBALB-Mock; Fig. 7 F). Together, these observations demonstrate that the NH_2-terminal domain of GRP94 recapitulates the activity of GRP94ΔKDEL in suppressing tumor growth and metastatic progression.

To compare the relative levels of GRP94ΔKDEL and GRP94 NTD secretion by 4T1 and KBALB cells, pulse-chase experiments were performed (Fig. 7 G). The level of GRP94ΔKDEL and GRP94 NTD secretion by both cell types was comparable, indicating that the tumor suppression observed after immunization did not reflect differences in GRP94 dose.

Tumor Histology. To gain insight into variations in the tumor microenvironment among the vaccination groups in the immunization and challenge protocol described above, tumors from the control and experimental groups were excised at the time of sacrifice, fixed, and prepared for histological analysis (Fig. 8). In all cases, 4T1 tumors were characterized by the predominance of malignant-appearing cells with hyperchromatic nuclei and high nuclear to cytoplasmic ratios (unpublished data). Mitotic figures were abundant and several atypical mitoses were observed, although the mitotic rate did not differ significantly among the various vaccination groups (unpublished data). The tumors featured large tracts of necrosis with obvious pyknosis and karyolysis of nuclear material (Fig. 8). At the midpoint of the study, tumors were characterized by the presence of macrophages, neutrophils, and rare lymphocytes, although the relative number of inflammatory cells did not differ greatly among the various vaccination groups (unpublished data). As seen at low power, tumors in control animals receiving vaccinations of PBS, mock-transfected 4T1 cells or mock-transfected NIH-3T3 cells were larger in size and contained larger areas of necrosis than tumors in animals re-

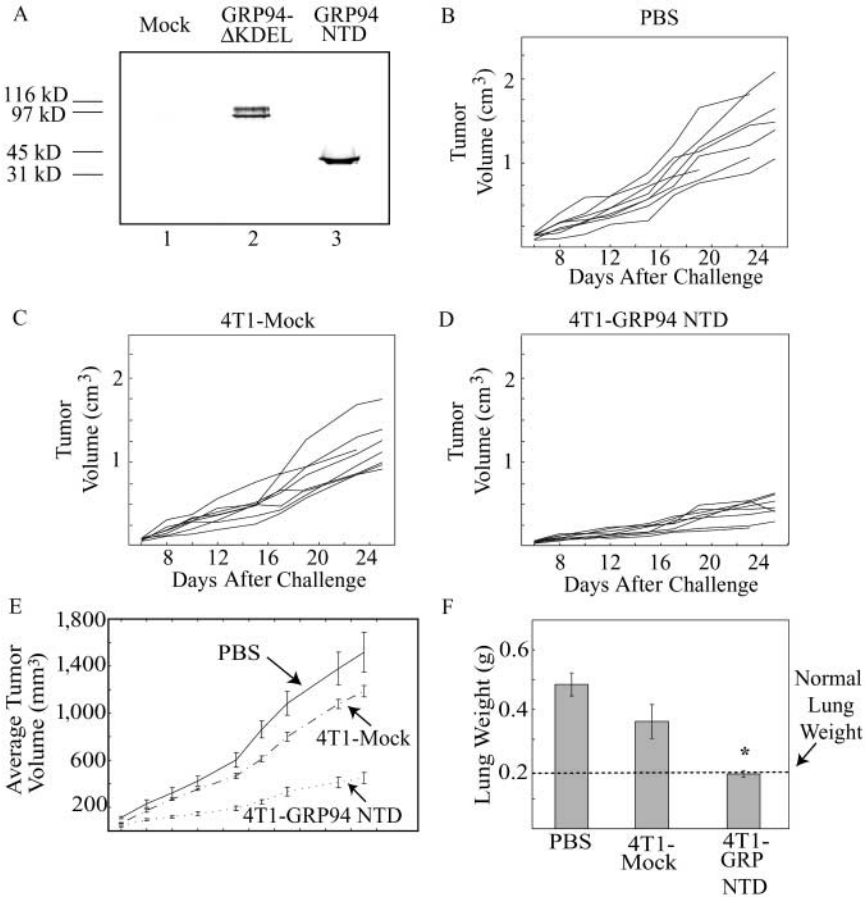

Figure 6. Vaccination with 4T1 mammary carcinoma cells secreting GRP94 NH_2-terminal domain leads to delayed tumor growth and decreased tumor metastasis. (A) Expression and secretion of GRP94 NTD by transfected 4T1 cells. 4T1 cells were transfected with either GRP94ΔKDEL or GRP94 NTD constructs or were mock-transfected (mock) as indicated. Cells were metabolically labeled with [^{35}S]Promix, and GRP94 domains were recovered from the media by immunoprecipitation before resolution by SDS-PAGE. Radiolabeled proteins were visualized by PhosphorImager analysis. (B–E) GRP94 NTD elicits delayed tumor growth rates. Female BALB/c mice were immunized with PBS or with irradiated, GRP94 NTD-transfected or irradiated, mock-transfected 4T1 cells as indicated. Animals were then challenged with unirradiated 4T1 cells and tumor volumes were followed over time, as described in Fig. 3. Tumor growth curves for individual mice are shown in B–D and average tumor volumes with standard error are shown in E. GRP94 NTD elicits decreased metastatic tumor progression. After animals were killed, lungs were resected from mice in B–D and weighed to determine the extent of metastatic tumor burden. Average lung weights with standard error are shown with groups differing significantly from PBS control denoted by an asterisk ($P \leq 0.00031$).

ceiving vaccinations of GRP94ΔKDEL of GRP94 NTD-transfected 4T1 or NIH-3T3 cells (Fig. 8).

Discussion

GRP94 can direct bound peptide antigens into the MHC class I cross-presentation pathway and displays natural adjuvant activity in its interactions with APCs (1, 7, 10, 13–15). This study explores the contribution of GRP94-bound antigens to the phenomenon of GRP94-mediated tumor suppression. In the experiments described, engineered GRP94/GRP94 domain-secreting cells served as the source of GRP94 immunizing activity. We observed that GRP94-mediated suppression of 4T1 tumor growth and metastatic progression was not tissue restricted, i.e., GRP94 secreted from allogenic (NIH-3T3) and syngeneic (KBALB) fibroblasts markedly inhibited the growth and metastasis of 4T1 breast carcinoma cells. That the effects of GRP94 were recapitulated by the GRP94 NTD, which lacks canonical peptide binding motifs, suggests that phenomenon other than peptide binding are of functional relevance to GRP94-mediated tumor suppression.

The observation that GRP94-mediated tumor suppression can be independent of the tissue of GRP94 origin was unexpected, particularly with respect to the broad literature implicating GRP94-bound peptide antigens in GRP94-elicited antitumor immune responses (1, 3, 10, 12). It has recently been discovered, however, that heat shock/chaperone proteins including GRP94 can alter immune function independent of bound tumor antigen composition. For example, GRP94 from nontumor sources elicits the phenotypic maturation of cells with up-regulation of cell surface costimulatory molecules and down-regulation of GRP94 receptors (14, 15). In addition, GRP94 stimulates IL-12, TNF-α, and IL-1β secretion from macrophages and DCs through activation of the NF-κB signaling pathway (14, 15). Such effects can be expected to influence the tumor microenvironment and antitumor immune responses. Thus, our data suggest that GRP94's role in tumor suppression may extend beyond the chaperoning of tumor peptides to APCs. In this light, it is interesting to note that GRP94 stimulation of CTL has been reported to occur regardless of the identity of bound peptide antigens (36, 37). In addition, in MHC class I–deficient *Xenopus* larvae, GRP94 elicits profound antitumor responses in a tumor antigen–independent manner (38).

As previously noted, and assuming that the two fibroblast cell lines used in this study share common immunodominant peptide epitopes with the 4T1 carcinoma, the data presented here remain compatible with models in which the GRP94 NH_2-terminal domain functions as a peptide binding site in addition to its established activity as an aden-

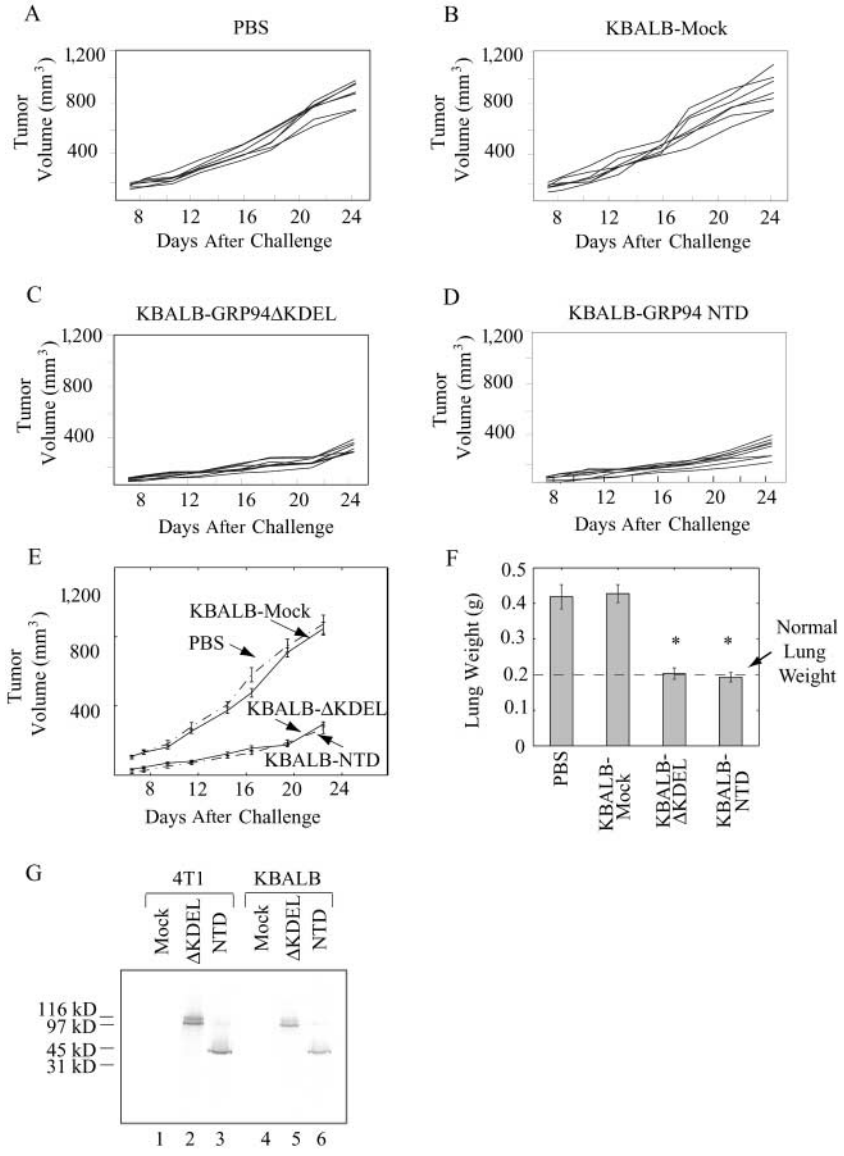

Figure 7. GRP94ΔKDEL and GRP94 NH_2-terminal domain secreted by syngeneic KBALB fibroblasts yield suppression of 4T1 tumor growth and metastasis. Female BALB/c mice were immunized with PBS or with irradiated, mock-transfected, GRP94ΔKDEL-transfected, or GRP94 NTD-transfected KBALB fibroblasts as indicated. Animals were then challenged with unirradiated 4T1 cells as described in Materials and Methods, and tumor volumes were followed over time. Tumor growth curves for individual mice in each group are shown in A–D and average tumor volumes with standard error are shown in E. (F) GRP94ΔKDEL or GRP94 NH_2-terminal domain secretion from K-BALB fibroblasts yields decreased tumor metastasis. After animals were killed, lungs were resected from mice as shown in A–E and weighed. Average weights with standard error are shown, with groups differing significantly from PBS control denoted by an asterisk ($P < 0.0003$ for KBALB-ΔKDEL and $P \leq 0.0002$ for KBALB-NTD). (G) Comparison of GRP94ΔKDEL and GRP94 NTD secretion by 4T1 and KBALB cells. Equal numbers (10^6 cells) of 4T1 KBALB cells were transfected with GRP94ΔKDEL (ΔKDEL samples), GRP94 NH_2-terminal domain (NTD samples) or mock-transfected (mock samples). 24 h after transfection, cells were metabolically labeled with [^{35}S]Promix and GRP94 species were recovered from the media by immunoprecipitation. Proteins were resolved by SDS-PAGE on 12.5% gels and visualized by PhosphorImager analysis.

osine nucleotide, geldanamycin, and radicicol binding site (33, 34). It should be considered, however, that recent studies have localized a putative GRP94 peptide binding site to the COOH terminus of the protein (35). In addition, crystallographic analyses of the Hsp90 NH_2-terminal adenosine nucleotide/geldanamycin binding domain did not identify peptide binding motifs analogous to those of Hsp70 chaperones, MHC class I or II molecules (33, 34, 35, 39). In addition, we report that the NH_2-terminal domain of GRP94 binds to APCs and modulates the phenotypic profile of DCs, consistent with a natural adjuvant function. Given these findings, we favor the interpretation that GRP94 NH_2-terminal domain function in tumor suppression is independent of bound peptides. Nonetheless, it remains formally possible that a previously uncharacterized motif capable of binding peptides suitable for expression on MHC class I resides in this domain. This possibility is under continuing investigation.

The ability of GRP94 and other heat shock proteins to elicit innate immune responses has recently been established (14–19). Hsp60, for example, binds Toll-like receptor-4 on macrophages, eliciting NF-κB signaling and the elaboration of TNF-α, IL-12, and IL-15 (18, 19). Hsp60 also directly elicits the activation of cytotoxic T lymphocytes, as indicated by the induction of interferon-γ secretion in the absence of bound tumor antigens (40). Similarly, Hsp70 binds to monocytes, initiating NF-κB signaling and the secretion of TNF-α, IL-1β, and IL-6 in a manner that is independent of the presence of chaperoned tumor antigen (16, 41, 42). In concert with these findings, it has recently been reported that GRP94 plays a key role in the folding and cell surface presentation of toll-like receptor 2 and 4 and that GRP94-mediated activation of DCs occurs through the same receptors (43, 44). Given the key role of toll-like receptors in the establishment of innate immune responses (20), it is likely that these interactions play a role in GRP94-mediated antitumor responses.

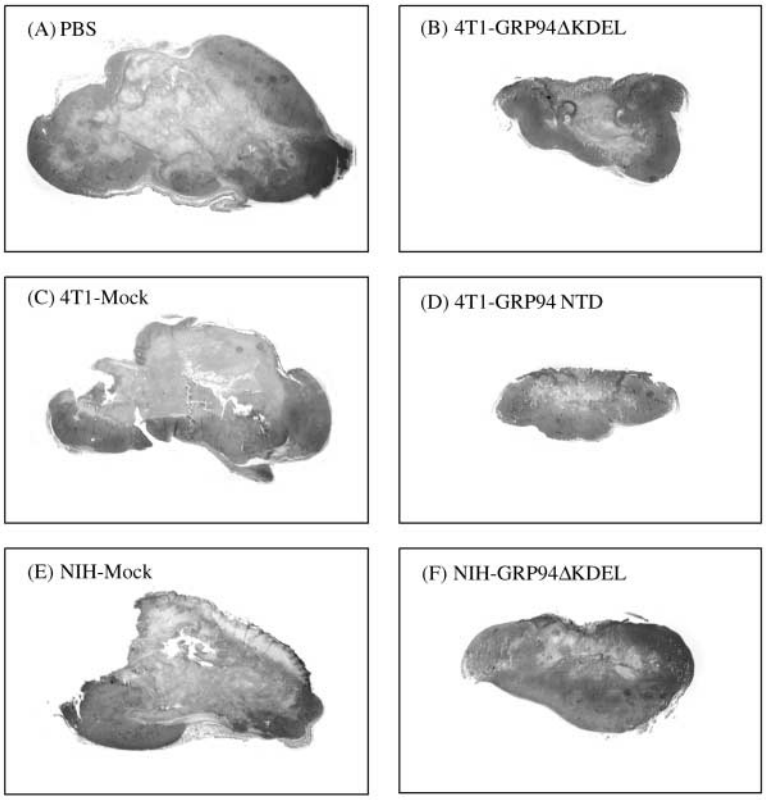

Figure 8. Vaccination with GRP94ΔKDEL- or GRP94 NTD-secreting 4T1 or NIH-3T3 cells yields smaller 4T1 tumor size and decreased intratumoral necrosis. Female BALB/c mice were immunized with PBS or with irradiated, GRP94ΔKDEL- or GRP94 NTD-secreting 4T1 or NIH-3T3 cells as described in Figs. 3 and 4. Animals were then challenged with unirradiated 4T1 cells. When the animals were killed, tumors were formalin fixed and paraffin-embedded specimens were sectioned and stained with hematoxylin and eosin. Representative tumor sections from each vaccination group are shown (2.5×). Tumors are from mice immunized with (A) PBS, (B) irradiated, GRP94ΔKDEL-transfected 4T1 cells, (C) irradiated, mock-transfected 4T1 cells, (D) irradiated, GRP94 NTD-transfected 4T1 cells, (E) irradiated, mock-transfected NIH-3T3 cells, or (F) irradiated, GRP94ΔKDEL-transfected NIH-3T3 cells.

The precise immunological mechanism whereby GRP94 secreted from fibroblasts mediates antitumor responses remains to be determined. To date, we have not detected the production of anti-4T1 CTL after our immunization protocol with GRP94-secreting fibroblasts (unpublished data), suggesting that the different GRP94 donor cells used in our experiments do not share common immunodominant antigens. Given recent proposals for an NK and NK T cell function in the suppression of tumor growth and metastasis and the demonstrations that interactions between NK cells and DCs can play a primary role in innate antitumor responses, it is tempting to speculate that NK and/or NK T cell activity might be responsive to GRP94 immunization, and thereby contribute to GRP94-mediated tumor suppression (45–51).

In mouse models of immunotherapy, a number of strategies have proven effective in the suppression of tumor growth and metastatic progression. Included in this growing list is the enhanced expression of cytokines (52, 53), costimulatory molecules (54, 55), or MHC class I molecules (56, 57) within tumor cells. It is likely that these strategies are effective by nature of their ability to enhance both innate and adaptive immune responses. We envision the introduction of secretory forms of GRP94, or the GRP94 NTD, to the animal as a similar vaccination strategy. In addition to the utilization of secreted GRP94–Fc fusion proteins (58), other novel approaches have been taken to introduce chaperones/heat shock proteins to the tumor microenvironment. For example, a transmembrane form of GRP94 has been expressed in tumor cells and been shown to elicit the maturation of DCs in vitro and tumor regression in vivo (59). Overexpression of Hsp70 within tumors has also been shown to result in tumor infiltration by DCs and the expression of Th1-promoting cytokines (17). In this context, secretion of heat shock proteins by cancer or noncancer cells may prove to be a useful adjuvant therapy in the treatment of cancer.

We thank Tianli Zheng for preparation of the GRP94ΔKDEL clone and Dr. Jeffrey Baker for guidance and advice on the generation of the GRP94 NTD domain. We are grateful to Karen Brinker and Delphine Malherbe for excellent technical advice regarding the DC experiments and Kwang Hu, Weip Chen, and Joshua Baker-LePain for technical assistance with tumor experiments. We also acknowledge Dan Ozaki and Shaza Fadel for their generous technical assistance with immunological assays. We are indebted to the Duke Histology Laboratory and to Dr. Mike Cook and Lynn Martinek of the Duke Comprehensive Cancer Center Flow Cytometry Facility. We express gratitude to Dr. Salvatore Pizzo, Dr. Brent Berwin, and Robyn Reed for critical comments on the manuscript.

This work was supported by the National Institutes of Health grant DK53058 to C.V. Nicchitta and by the National Institutes of Health Medical Scientist Training Program grant T32GM-07171 to J.C. Baker-LePain.

Submitted: 19 March 2002
Revised: 17 September 2002
Accepted: 11 October 2002

References

1. Srivastava, P.K. 2002. Interaction of heat shock proteins with peptides and antigen presenting cells: chaperoning of the in-

nate and adaptive immune responses. *Annu. Rev. Immunol.* 20:395–425.
2. Srivastava, P.K., A.B. DeLeo, and L.J. Old. 1986. Tumor rejection antigens of chemically induced sarcomas of inbred mice. *Proc. Natl. Acad. Sci. USA.* 83:3407–3411.
3. Blachere, N.E., H. Udono, S. Janetzki, Z. Li, and P.K. Srivastava. 1993. Heat shock protein vaccines against cancer. *J. Immunother.* 14:352–356.
4. Tamura, Y., P. Peng, K. Liu, M. Daou, and P.K. Srivastava. 1997. Immunotherapy of tumors with autologous tumor-derived heat shock protein preparations. *Science.* 278:117–120.
5. Srivastava, P.K., and M. Heike. 1991. Stress-induced proteins in immune response to cancer. *Curr. Top. Microbiol. Immunol.* 167:109–123.
6. Spee, P., and J. Neefjes. 1997. TAP-translocated peptides specifically bind proteins in the endoplasmic reticulum, including gp96, protein disulfide isomerase, and calreticulin. *Eur. J. Immunol.* 27:1685–1690.
7. Singh-Jasuja, H., R.E.M. Toes, P. Spee, C. Munz, N. Hilf, S.P. Schoenberger, P. Riccardi-Castagnoli, J. Neefjes, H.G. Rammensee, D. Arnold-Schild, et al. 2000. Cross-presentation of glycoprotein 96–associated antigens on major histocompatibility complex class I molecules requires receptor-mediated endocytosis. *J. Exp. Med.* 191:1965–1974.
8. Wassenberg, J.J., C. Dezfulizan, and C.V. Nicchitta. 1999. Receptor mediated and fluid phase pathways for internalization of the ER hsp90 chaperone GRP94 in murine macrophages. *J. Cell Sci.* 112:2167–2175.
9. Arnold-Schild, D., D. Hanau, D. Spehner, C. Schmid, H.G. Rammensee, H. de la Salle, and H. Schild. 1999. Cutting edge: receptor-mediated endocytosis of heat shock proteins by professional antigen-presenting cells. *J. Immunol.* 162: 3757–3760.
10. Binder, R.J., D.K. Han, and P.K. Srivastava. 2000. CD91: a receptor for heat shock protein gp96. *Nat. Immunol.* 2:151–155.
11. Castellino, F., P.E. Boucher, K. Eichelberg, M. Mayhew, J.E. Rothman, A.N. Houghton, and R.N. Germain. 2000. Receptor-mediated uptake of antigen/heat shock protein complexes results in major histocompatibility complex class I antigen presentation via two distinct processing pathways. *J. Exp. Med.* 191:1957–1964.
12. Suto, R., and P.K. Srivastava. 1995. A mechanism for the specific immunogenicity of heat shock protein-chaperoned peptides. *Science.* 269:1585–1588.
13. Berwin, B., M.F.N. Rosser, K.G. Brinker, and C.V. Nicchitta. 2002. Transfer of GRP94(gp96)-associated peptides onto endosomal MHC Class I molecules. *Traffic.* 3:358–366.
14. Singh-Jasuja, H., H.U. Scherer, N. Hilf, D. Arnold-Schild, H.G. Rammensee, R.E. Toes, and H. Schild. 2000. The heat shock protein gp96 induces maturation of dendritic cells and down-regulation of its receptor. *Eur. J. Immunol.* 30:2211–2215.
15. Basu, S., R.J. Binder, R. Suto, K.M. Anderson, and P.K. Srivastava. 2000. Necrotic but not apoptotic cell death releases heat shock proteins, which deliver a partial maturation signal to dendritic cells and activate the NF-kappa B pathway. *Int. Immunol.* 12:1539–1546.
16. Asea, A., S.K. Kraeft, E.A. Kurt-Jones, M.A. Stevenson, L.B. Chen, R.W. Finberg, G.C. Koo, and S.K. Calderwood. 2000. HSP70 stimulates cytokine production through a CD14-dependent pathway, demonstrating its dual role as a chaperone and cytokine. *Nat. Med.* 6:435–442.
17. Todryk, S., A. Melchner, N. Hardwock, E. Linardakis, A. Bateman, M. Colombo, A. Stoppacciaro, and R. Vile. 1999. Heat shock protein 70 induced during tumor killing induces Th1 cytokines and targets immature dendritic cell precursors to enhance antigen uptake. *J. Immunol.* 163:1398–1408.
18. Kol, A., A.H. Lichtman, R.W. Finberg, P. Libby, and E.A. Kurt-Jones. 2000. Cutting edge: heat shock protein (HSP) 60 activates the innate immune response: CD14 is an essential receptor for HSP60 activation of mononuclear cells. *J. Immunol.* 164:13–17.
19. Ohashi, K., V. Burkart, S. Flohe, and H. Kolb. 2000. Cutting edge: heat shock protein 60 is a putative endogenous ligand of the toll-like receptor 4-complex. *J. Immunol.* 164:558–561.
20. Janeway, C.A., and R. Medzhitov. 2002. Innate immune recognition. *Annu. Rev. Immunol.* 20:197–216.
21. Harlow, E., and D. Lane. 1988. Antibodies: A Laboratory Manual. Cold Spring Harbor Laboratory, Cold Spring Harbor, New York. 726 pp.
22. Haynes, R.L., T. Zheng, and C.V. Nicchitta. 1997. Structure and folding of nascent polypeptide chains during protein translocation in the endoplasmic reticulum. *J. Biol. Chem.* 272:17126–17133.
23. Wearsch, P.A., and C.V. Nicchitta. 1996. Purification and partial molecular characterization of GRP94, an ER resident chaperone. *Protein Expr. Purif.* 7:114–121.
24. Inaba, K., M. Inaba, N. Romani, H. Aya, M. Deguchi, S. Ikehara, S. Muramatsu, and R.M. Steinman. 1992. Generation of large numbers of dendritic cells from mouse bone marrow cultures supplemented with granulocyte/macrophage colony-stimulating factor. *J. Exp. Med.* 176:1693–1702.
25. Kornberg, A. 1990. Why purify enzymes? *Methods Enzymol.* 182:1–5.
26. Reed, R.C., T. Zheng, and C.V. Nicchitta. 2002. GRP94-associated enzymatic activities: resolution by chromatographic fractionation. *J. Biol. Chem.* 277:25082–25089.
27. Baker-LePain, J.C., R.C. Reed, and C.V. Nicchitta. 2002. ISO: a critical evaluation of the role of peptides in heat shock/chaperone protein-mediated tumor rejection. *Curr. Opin. Immunol.* In press.
28. Munro, S., and H.R.B. Pelham. 1987. A C-terminal signal prevents secretion of lumenal ER proteins. *Cell.* 48:899–907.
29. Peter, F., V.P. Nguyen, and H.D. Soling. 1992. Different sorting of Lys-Asp-Glu-Leu proteins in rat liver. *J. Biol. Chem.* 267:10631–10637.
30. Aslakson, C.J., and F.R. Miller. 1992. Selective events in the metastatic process defined by analysis of the sequential dissemination of subpopulations of a mouse mammary tumor. *Cancer Res.* 52:1399–1405.
31. Wearsch, P.A., and C.V. Nicchitta. 1996. Endoplasmic reticulum chaperone GRP94 subunit assembly is regulated through a defined oligomerization domain. *Biochemistry.* 35: 16760–16769.
32. Rosser, M.F.N., and C.V. Nicchitta. 2000. Ligand interactions in the adenosine nucleotide binding domain of the hsp90 chaperone, GRP94. I. Evidence for allosteric regulation of ligand binding. *J. Biol. Chem.* 275:22806–22814.
33. Prodromou, C., S.M. Roe, R. Obrien, J.E. Ladbury, P.W. Piper, and L.H. Pearl. 1997. Identification and structural characterization of the N-terminal domain of the ATP/ADP-binding site in the hsp90 molecular chaperone. *Cell.* 90:65–75.
34. Stebbins, C.E., A.A. Russo, N. Rosen, F.U. Hartl, and N.P. Pavletich. 1997. Crystal structure of an Hsp90-geldanamycin

complex: targeting of a protein chaperone by an anti-tumor agent. *Cell.* 89:239–250.
35. Linderoth, N.A., A. Popowicz, and S. Sastry. 2000. Identification of the peptide-binding site in the heat shock chaperone/tumor rejection antigen gp96 (Grp94). *J. Biol. Chem.* 275:5472–5477.
36. More, S., M. Breloer, B. Fleischer, and A. von Bonin. 1999. Activation of cytotoxic T cells in vitro by recombinant gp96 fusion proteins irrespective of the "fused" antigenic peptide sequence. *Immunol. Lett.* 69:275–282.
37. Breloer, M., B. Fleischer, and A. von Bonin. 1999. In vivo and in vitro activation of T cells after administration of Ag-negative heat shock proteins. *J. Immunol.* 162:3141–3147.
38. Robert, J., J. Gantress, L. Rau, A. Bell, and N. Cohen. 2002. Minor histocompatibility antigen-specific MHC-restricted CD8 T cell responses elicited by heat shock proteins. *J. Immunol.* 168:1697–1703.
39. Zhu, X., X. Zhao, W.F. Burkholder, A. Gragerov, C.M. Ogata, M.E. Gottesman, and W.A. Hendrickson. 1996. Structural analysis of substrate binding by the molecular chaperone DnaK. *Science.* 272:1606–1614.
40. More, S.H., M. Breloer, and A. von Bonin. 2001. Eukaryotic heat shock proteins as molecular links in innate and adaptive immune responses: Hsp60-mediated activation of cytotoxic T cells. *Int. Immunol.* 13:1121–1127.
41. Asea, A., E. Kabingu, M.A. Stevenson, and S.K. Calderwood. 2000. HSP70 peptide-bearing and peptide-negative preparations act as chaperokines. *Cell Stress Chaperones.* 5:425–431.
42. Huang, Q., J.F.L. Richmond, K. Suzue, H.N. Eisen, and R.A. Young. 2000. In vivo cytotoxic T lymphocyte elicitation by mycobacterial heat shock protein 70 fusion proteins maps to a discrete domain and is $CD4^+$ T cell independent. *J. Exp. Med.* 191:403–408.
43. Randow, F., and B. Seed. 2001. Endoplasmic reticulum chaperone gp96 is required for innate immunity but not cell viability. *Nat. Cell Biol.* 3:891–896.
44. Ramunas, M.V., S. Braedel, N. Hilf, H. Singh-Jasuja, S. Herter, P. Ahmad-Nejad, C.J. Kirschning, C. da Costa, H. Rammensee, H. Wagner, et al. 2002. The endoplasmic reticulum-resident heat shock protein gp96 activtes dendritic cells via the toll-like receptor 2/4 pathway. *J. Biol. Chem.* 277: 20847–20853.
45. Talmadge, J.E., K.M. Meyers, D.J. Prieur, and J.R. Starkey. 1980. Role of NK cells in tumor growth and metastasis in beige mice. *Nature.* 284:622–624.
46. Crowe, N.Y., M.J. Smyth, and D.I. Godfrey. 2002. A critical role for natural killer T cells in immunosurveillance of methylcholanthrene-induced sarcomas. *J. Exp. Med.* 196:119–127.
47. Cui, J., T. Shin, T. Kawano, H. Sato, E. Kondo, I. Toura, Y. Kaneko, H. Koseki, M. Kanno, and M. Taniguchi. 1997. Requirement for Vα14 NKT cells in IL-12-mediated rejection of tumors. *Science.* 278:1623–1626.
48. Hashimoto, W., K. Takeda, R. Anzai, K. Ogasawara, H. Sakihara, K. Sugiura, S. Seki, and K. Kumagai. 1995. Cytotoxic NK1.1 Ag^+ αβ T cells with intermediate TCR induced in the liver of mice by IL-12. *J. Immunol.* 165:2665–2670.
49. Toura, I., T. Kawano, Y. Akutsu, T. Nakayama, T. Ochiai, and M. Taniguchi. 1999. Cutting edge: inhibition of experimental tumor metastasis by dendritic cells pulsed with α-galactosylceramide. *J. Immunol.* 163:2387–2391.
50. Zitvogel, L. 2002. Dendritic and natural killer cells cooperate in the control/switch of innate immunity. *J. Exp. Med.* 195: F9–F14.
51. Fernandez, N.C., A. Lozier, C. Flament, P. Ricciardi-Castagnoli, D. Bellet, M. Sutter, M. Perricaudet, T. Tursz, E. Maraskovsky, and L. Zitvogel. 1999. Dendritic cells directly trigger NK cell functions: a cross-talk relevant in innate anti-tumor immune responses in vivo. *Nat. Med.* 5:405–411.
52. Dranoff, G., E. Jaffee, A. Lazenby, P. Golumbek, H. Levitsky, K. Brose, V. Jackson, H. Hamada, D. Pardoll, and R.C. Mulligan. 1993. Vaccination with irradiated tumor cells engineered to secrete murine granulocyte-macrophage colony-stimulating factor stimulates potent, specific, and long-lasting anti-tumor immunity. *Proc. Natl. Acad. Sci. USA.* 90: 3539–3543.
53. Marincola, F.M., S. Ettinghausen, P.A. Cohen, L.B. Cheshire, N.P. Restifo, J.J. Mule, and S.A. Rosenberg. 1994. Treatment of established lung metastases with tumor-infiltrating lymphocytes derived from a poorly immunogenic tumor engineered to secrete human TNF-alpha. *J. Immunol.* 152: 3500–3513.
54. Chen, L., S. Ashe, W.A. Brady, I. Hellstrom, K.E. Hellstrom, J.A. Ledbetter, P. McGowan, and P.S. Linsley. 1992. Costimulation of antitumor immunity by the B7 counterreceptor for the T lymphocyte molecules CD28 and CTLA-4. *Cell.* 71:1093–1102.
55. Townsend, S.E., and J.P. Allison. 1993. Tumor rejection after direct costimulation of $CD8^+$ T cells by B7-transfected melanoma cells. *Science.* 259:368–370.
56. Hui, K., F. Gosveld, and H. Festenstein. 1984. Rejection of transplantable AKR leukaemia cells following MHC DNA-mediated cell transformation. *Nature.* 311:750–752.
57. Tanaka, K., E. Gorelik, M. Watanabe, N. Hozumi, and G. Jay. 1988. Rejection of B16 melanoma induced by expression of a transfected major histocompatibility complex class I gene. *Mol. Cell. Biol.* 8:1857–1861.
58. Yamazaki, K., T. Nguyen, and E.R. Podack. 1999. Cutting edge: tumor secreted heat shock-fusion protein elicits CD8 cells for rejection. *J. Immunol.* 163:5178–5182.
59. Zheng, H., J. Dai, D. Stoilova, and Z. Li. 2001. Cell surface targeting of heat shock protein gp96 induces dendritic cell maturation and antitumor immunity. *J. Immunol.* 167:6731–6735.